DIFFRACTION IMAGES OF TRUNCATED PERIODIC OBJECTS IN PANORAMIC CAMERAS IN THE PRESENCE OF PARABOLIC IMAGE MOTION

A. K. GUPTA AND K. SINGH*

Department of Physics, Indian Institute of Technology, New Delhi 110 029

ABSTRACT

Irradiance distribution in the diffraction images of truncated one-dimensional periodic targets formed in the presence of parabolic image motion is discussed. Incoherent objects with sine and square wave profiles are considered in the case of an optical system with circular aperture. Image contrast, tabulated for a number of cases, is expected to provide a valuable tool for an image analyst.

INTRODUCTION

USE of optical transfer function techniques in image evaluation is now very well known and an excellent review of the present status of the subject has been given by Norton[1]. Truncated periodic targets are also useful in many practical situations, when these occur in image format in connection with the detection and resolution in aerial photographs of a wide variety of objects. Consequently the diffraction images of truncated targets have been investigated extensively[2-5].

Despite the best image motion compensation (IMC) techniques, some residual motion is always present[6-9] and this impairs the quality of aerial photographs. Effects of linear and sinusoidal motion on the images of various objects has been extensively investigated[3-5,7] in the past. Residual image motion in transverse scanning panoramic cameras[7,10] results from the finite slit width which precludes film's IMC from being exactly correct for all images simultaneously exposed in the slit. The image displacement is a parabolic function of time[7,10-12]. Such motion has recently been considered with respect to its effect on imagery of infinite periodic objects[13], holographic measurements[14] and image restoration[15,16].

The present paper discusses some aspects of diffraction images of truncated objects in the presence of parabolic image motion.

2. THEORY

The frequency spectra $I(\omega)$ of the image and $O(\omega)$ of the object are related by

$$I(\omega) = O(\omega) . T(\omega) \tag{1}$$

where $T(\omega)$ is the system transfer function and ω the normalised spatial frequency. The intensity distribution $i(v)$ in the image is then given by

$$i(v) = \int_{-\infty}^{\infty} T(\omega).O(\omega). \exp(iv\omega)\, d\omega \tag{2}$$

The object intensity function for N-cycle bar and sinusoidal targets are given respectively[2,4], by

$$O(\omega) = (2\pi\omega)^{-1} [\sin(2N\omega L)/\cos(\omega L)] \tag{3}$$

$$O(\omega) = \pi/2\omega . \sin(2N\omega L)/(\pi^2 - 4\omega^2 L^2) \tag{4}$$

where 4 L is the spatial period. Both v and L are in reduced units.

The overall optical transfer function $T(\omega)$ of the optical system under consideration is the product of incoherent transfer function $C(\omega)$ of the diffraction limited system and the transfer function $t(\omega)$ for the image motion, *i.e.*

$$T(\omega) = C(\omega) . t(\omega) \tag{5}$$

$C(\omega)$ for the diffraction limited circular aperture is given by

$$C(\omega) = 2/\pi [\cos^{-1}(\omega/2) - \omega/2 (1-\omega^2/4)^{\frac{1}{2}}] \tag{6}$$

The OTF, for parabolic image motion is given[7,10,11] by

$$t(\omega) \frac{\sqrt{I_1^2 + I_2^2}}{2\sqrt{\omega A}} . e^{\theta'} \tag{7}$$

Here $\theta' = \tan^{-1}(I_2/I_1)$ is the phase log and I_1 and I_2 are Fresnel integrals given by

$$I_1 = \int_0^{2\sqrt{\omega A}} \cos(\pi/2u^2)\, du.$$

$$I_2 = \int_0^{2\sqrt{\omega A}} \sin(\pi/2u^2)\, du.$$

A is the dimensionless motion parameter equal to $Bt_e^2/\lambda F$. Here B is defined by the equation of parabolic motion[7], t_e is the total exposure time, λ is the wavelength of the incident light and F is the *f*-number of the optical system.

3. RESULTS AND DISCUSSIONS

Figures 1 (*a*) to 1 (*c*) show the intensity distribution in the diffraction images of square wave targets for N = 3, 7 and 15 for various values of A. Similar curves have been plotted in case of sinewave objects and are illustrated in Figs. 2 (*a*) to 2 (*c*). Image in the absence of motion, *i.e.*, (A = 0·0) are shown in all figures by dotted

---

* To whom all correspondence may please be addressed.

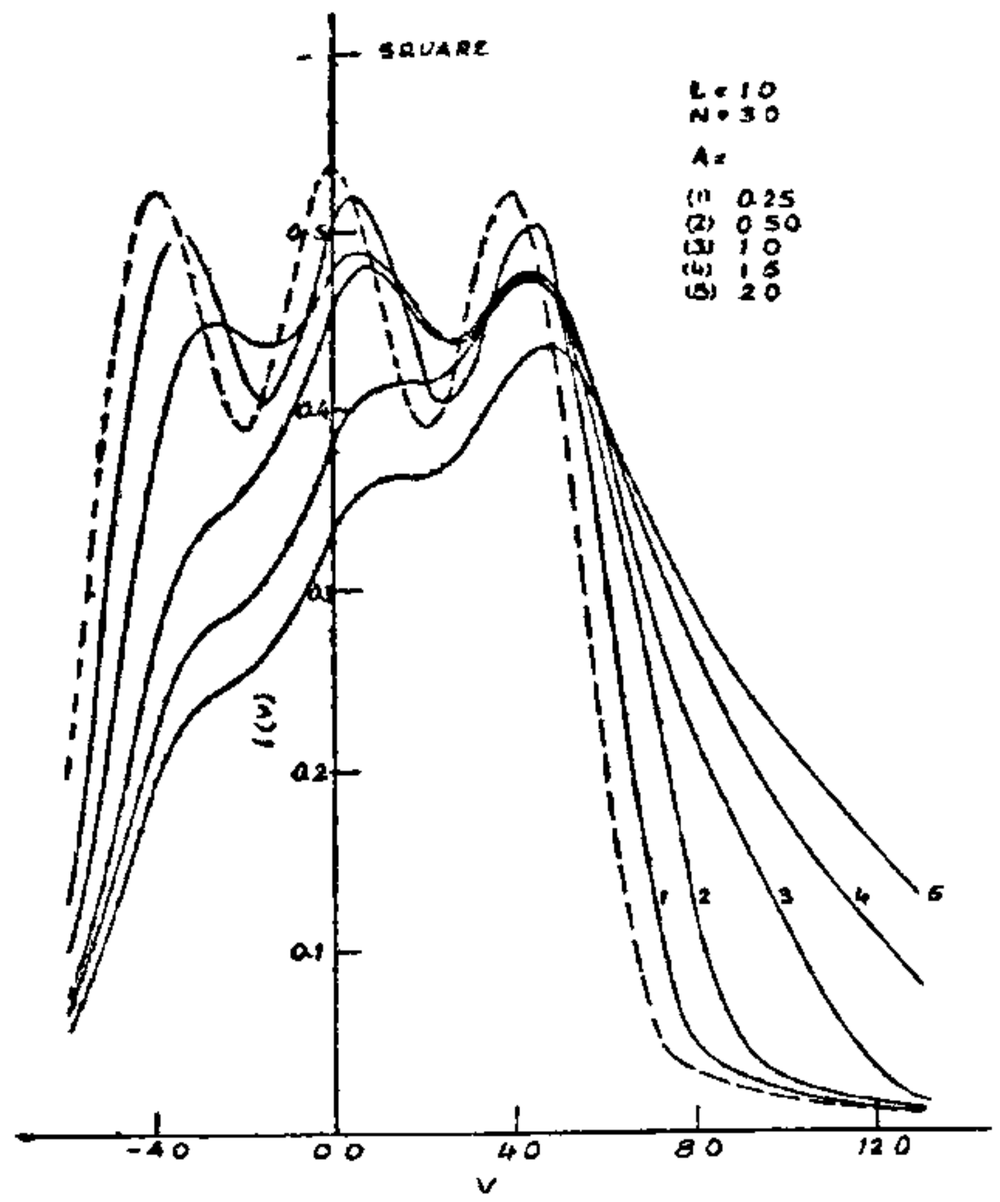

FIG. 1 (*a*). Diffraction Images of square wave object in presence of parabolic image motion. (A = 0·0, 0·25, 0·5, 1·0, 1·5 and 2·0, N = 3·0 and L = 1·0).

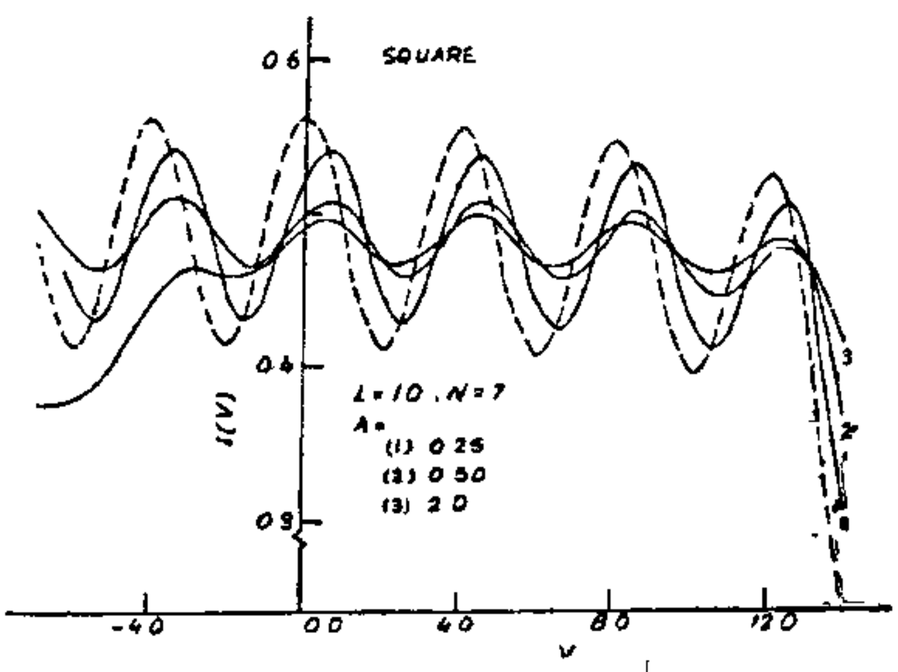

FIG. 1 (*b*). Same as 1 (*a*) with N = 7 and A = 0·0, 0·25, 0·50 and 2·0.

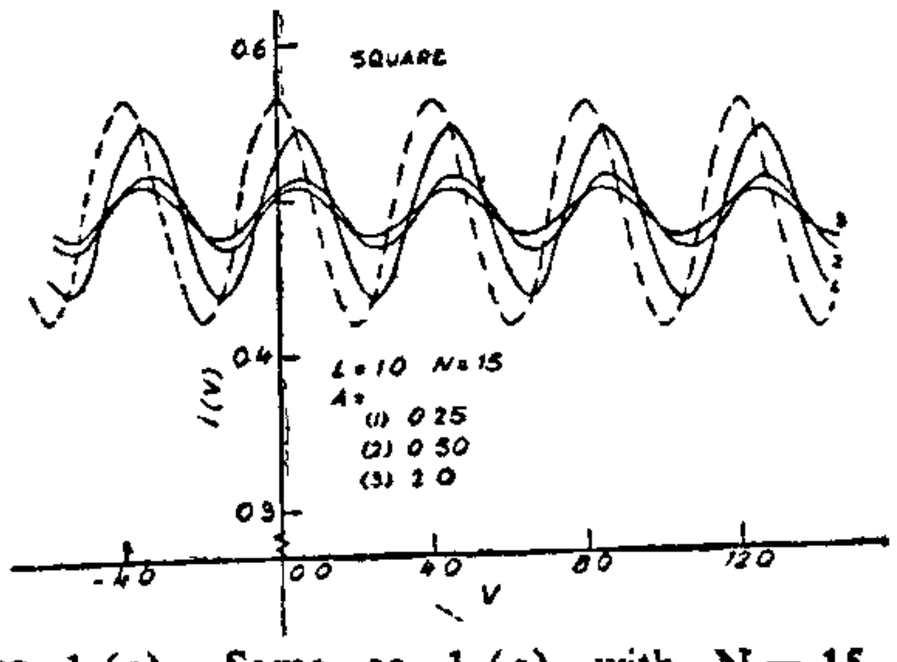

FIG. 1 (*c*). Same as 1 (*a*) with N = 15 and A = 0·0, 0·25, 0·50 and 2·0.

curves and these agree with the results published by Barakat and Lerman[2].

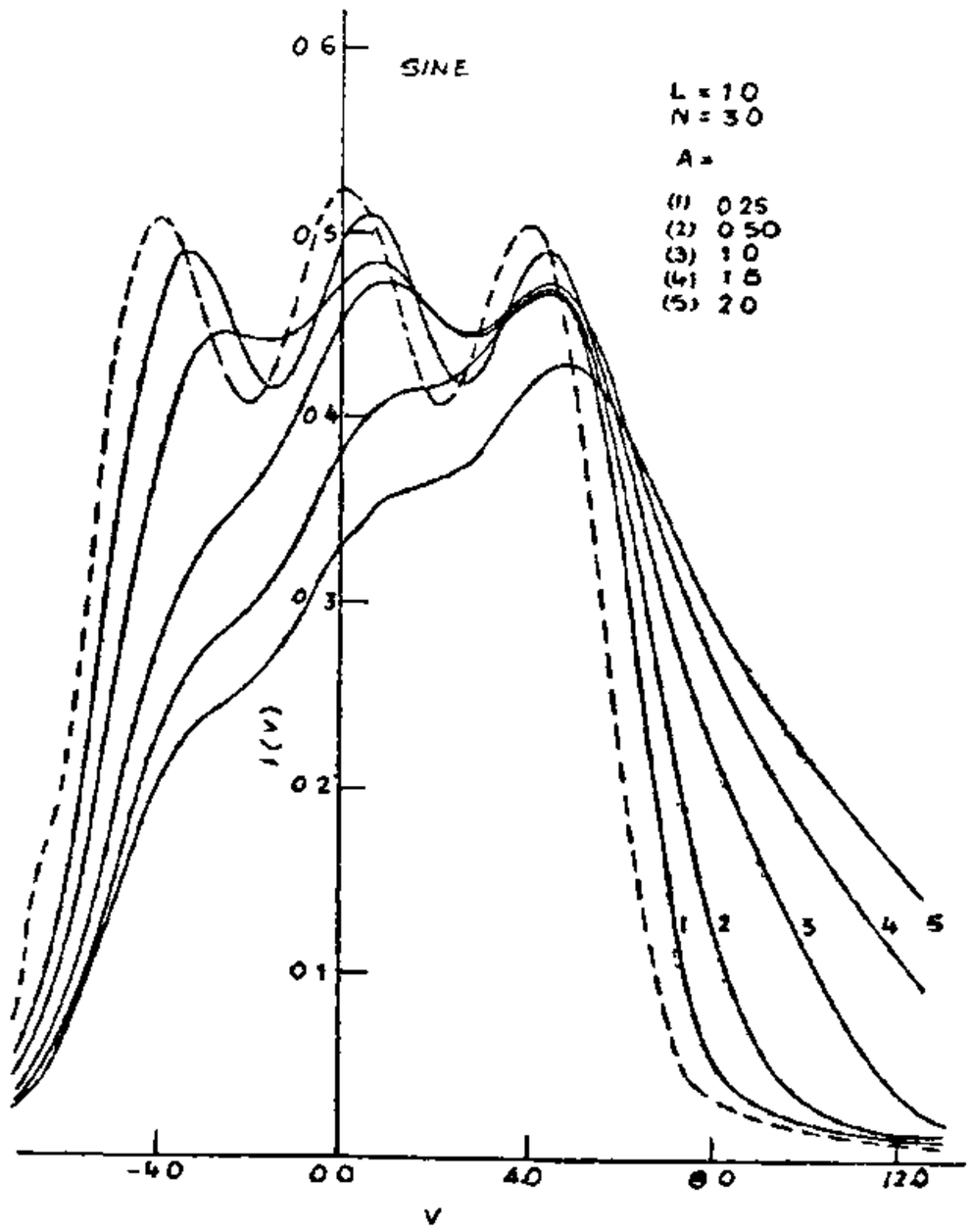

FIG. 2 (*a*). Diffraction images of sine wave object in the presence of parabolic image motion. (A = 0·0, 0·25, 0·5, 1·0, 1·5 and 2·0, N = 3·0 and L = 1·0).

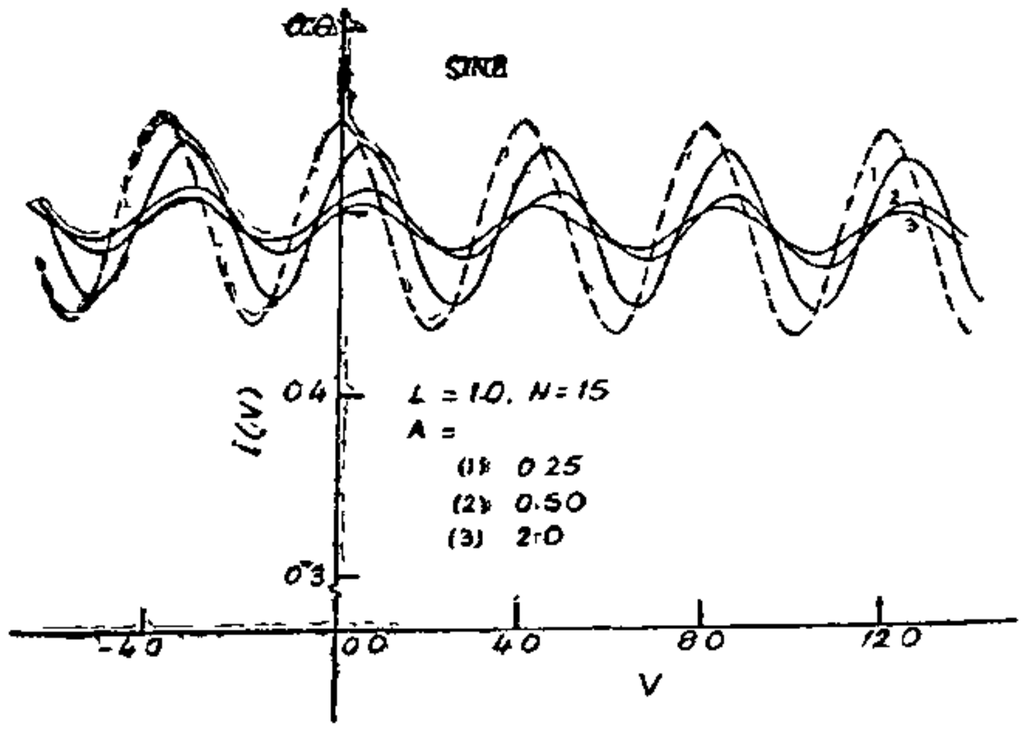

FIG. 2 (*b*). Same as 2 (*a*) with N = 7 and A = 0·0, 0·25, 0·5 and 2·0.

Square wave targets are imaged with higher contrast as compared to the sine wave targets. However, the general trend of results in the case of sine and square wave objects is very similar. It is evident from Figs. 1 and 2 that peak intensity position is shifted in presence of motion. The shift is, however, constant beyond A = 0·5. It is explained on the basis of the fact that the phase part of the transfer function becomes oscillatory beyond a certain value of ω for given value of

A (For examples at $\omega = 0{\cdot}7$, for $A = 1{\cdot}0$) and then becomes constant afterwards in high frequency region. It is also seen that the intensity distribution is asymmetric with respect to origin. Such asymmetry is also observed in investigating the comatic images by Ingelstam, *et al.*[17], and Barakat[18].

It is obvious from Figs. 1 and 2 that the contrast is reduced in presence of parabolic motion, hence a degradation of image is caused. Degradation is increased as the value of A increases. The average irradiance in the central portion of the image is increased as N increases and approaches $0{\cdot}50$ as N approaches ∞. It must also be observed that there is no reversal of contrast for any value of A. There is no loss of periodicity for moderate values of A, *e.g.*, for $A = 0{\cdot}5$, $1{\cdot}0$ for $N = 3$, and 5. Some loss of periodicity results for higher values of A.

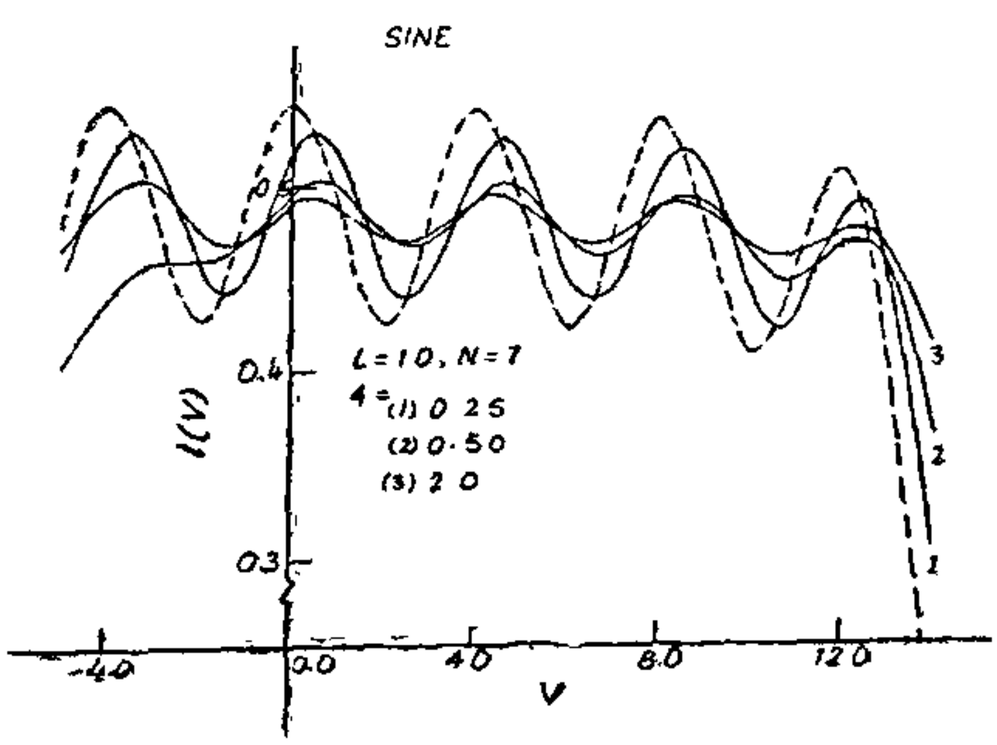

FIG. 2 (*c*). Same as 2 (*a*) with N = 15 and A = $0{\cdot}0$, $0{\cdot}25$, $0{\cdot}5$ and $2{\cdot}0$.

Table I gives a better idea of the effect of motion on the image quality of targets under consideration. The method used for calculating modulation and average irradiance is as outlined in our previous papers[3,4]. It is inferred that the effect of image motion is practically nil on the average irradiance compared to the enormous changes in the modulation and hence modulation is ultimate tool to decide how many cycles are required for the approximation of an infinite sine wave target.

Additional Remarks :

In this paper we confined ourselves to one-dimensional objects. We would also like to mention that the motion degraded images of two-dimensional objects such as disks, annulas, etc., cannot be calculated using Eqn. 6 for the OTF of the total system does not posses a rotational symmetry but acquires a certain azimuthal dependence. Work in this context has been done by Rattan and Singh[19].

TABLE 1

Modulation in the diffraction images of square and sine wave targets

A/N	3	5	7	9	11	13	15
			SQUARE WAVE				
0·0	·1532	·1518	·1515	·1504	·1491	·1495	·1492
0·25	·1136	·1143	·1142	·1136	·1125	·1129	·1127
0·50	·0641	·0479	·0482	·0483	·0474	·0446	·0454
1·0	..	0·450	·0453	·0455	·0446	·0454	·0451
1·5	..	..	·0396	·0396	·0392	·0396	·0394
2·0	..	..	·0299	·0302	·0299	·0296	·0301
			SINE				
0·0	·1189	·1190	·1188	·1180	·1170	·1174	·1172
0·25	·0878	·0895	·0896	·0893	·0883	·0887	·0885
0·50	·0339	·0374	·0377	·0380	·0372	·0376	·0377
1·0	..	·0352	·0355	·0356	·0349	·0356	·0355
1·5	..	..	·0309	·0312	·0309	·0312	·0308
2·0	..	..	·0233	·0237	·0235	·0237	·0236

It is also interesting to include the effect of lens-film combination on the diffraction images. It can be done by cascading the Film's MTF with the system MTF's provided the linear processes would be involved. However, complexity arises due to some non-linear phenomena involved during the exposure and development of the film.

We have considered in our calculation unit contrast truncated targets so that object contrast bears a linear relationship with image contrast. It is interesting to estimate the error caused by truncation by varying the modulation. For modulation less than unity there is non-linear relationship[20] between object and image contrast.

1. Norton, C. L., *Photogramm. Eng*, 1975, 41, 203.
2. Barakat, R. and Lerman, S., *Appl. Opt.*, 1967, 6, 545.
3. Singh, K. and Jain, N. K., *Nouv. Rev. Opt.*, 1972, 6, 309.
4. —, Rattan, R. and Jain, N. K., *Appl. Opt.*, 1973, 12, 1846.
5. —, Jain, N. K. and Rattan, R., *Atti. Fond. G. Ronchi.*, 1973, 28, 545.
6. Nagel, M. R., *Evaluation of Motion Degraded Images,* Proc. of a Seminar held in Cambridge, Mass., Dec. 3–5, 1968, (NASA, Washington, DC. 1969).
7. Jensen, N, *Optical and Photographic Reconnaissance. System,* John Wiley and Sons, New York, 1968.
8. Dubovik, A. S., *Photographic Recording of High Speed Process,* Bergamon Press, Oxford, 1968.
9. Fouche', G., In : *Space Optics,* Eds., Maréchal, A. and Courtes, G, Gordon and Breach Science, Publ. N.Y., 1974, p. 374.
10. Rosenau, M. D., *J. Photogram. Eng*, 1961, 27, 421.
11. Som, S. C., *J. Opt. Soc. Am*, 1971, 61, 859.
12. Wolf, P. R., *Elements of Photogrammetry,* McGraw-Hill Book Co., N.Y., 1974.
13. Rattan, R. and Singh, K., *Atti. Fond. G. Ronchi.*, 1972, 27, 727.
14. Gupta, P. C. and Singh, K., *Pramāna,* 1974, 3, 390.
15. Jablonwski, D. P. and Singh, H., *Lee. Appl. Opt.*, 1973, 12, 703.
16. Sawchuk, A. A, *Proc. IEEE,* 1972, 60, 854.
17. Inglestam, E. *et al., J. Opt. Soc. Am.,* 1956, 46, 767.
18. Barakat, R. and Houston, A., *Ibid.,* 1965, 55, 1142.
19. Rattan, R. and Singh, K., *Nouv. Rev. Opt.*, 1975, 6, in press.
20. Jaiswal, A. K. and Bhusan, *J. Appl. Opt*, 1974, 13, 1839.

CHEMICAL COMPONENTS OF *ASPLENIUM LACINIATUM*

R. B. GUPTA, R. N. KHANNA AND N. N. SHARMA
Department of Chemistry, University of Delhi, Delhi 110 007

ABSTRACT

Asplenium laciniatum has been found to contain octatriacontane, stearic acid, vitamin-K_2, phthiocol, β-sitosterol and β-sitosterol D-O-glucoside. The free sugars identified are sucrose (large amount), glucose, galactose and arabinose. This is the first report of the isolation of vitamin-K_2 and phthiocol from a plant source.

ASPLENIUM laciniatum is a fern belonging to the group of highly advanced cryptogens. Its alcoholic or acetone extract has a burning effect on the skin and produce a wound which takes about ten days to heal. Investigation of the chemical components was taken up in order to find out the active principles present in it.

The dried plant (4 Kg) obtained from Kalimpong (West Bengal) was exhaustively extracted with acetone and alcohol successively. Acetone from the acetone extract was removed under reduced pressure and the residue adsorbed on silica gel and chromatographed over a column of silica gel whereby the following compounds were obtained.

Compound A, eluted with petroleum ether, m.p. 68–70° (200 mg, from ethyl acetate). Its I.R. spectrum showed it to be aliphatic in nature. It did not answer Liebermann–Burchard test and moved along the solvent front on TLC in *n*-hexane. The mass spectrum showed a mass peak at m/e 534 and a cluster of peaks at 14 units ($-CH_2$) apart. The highest peak in each cluster represented C_nH_{2n+1} fragment which was accompanied by C_nH_{2n} and C_nH_{2n-1} peaks. Intense peaks were for C–4 and C–5 units and fragment intensity decreased in a smooth curve down to ($M^+-C_2H_5$). The (M^+-CH_3) peak was very weak. It was identified as octatriacontane.